IEEE Photonics Journal
An IEEE Photonics Society Publication

Open Access

Broadband 1 × 3 Couplers With Variable Splitting Ratio Using Cascaded Step-Size MMI

Volume 10, Number 3, June 2018

Ye Tian
Jifang Qiu
Mingbin Yu
Zhuili Huang
Yingying Qiao
Zhenli Dong
Jian Wu

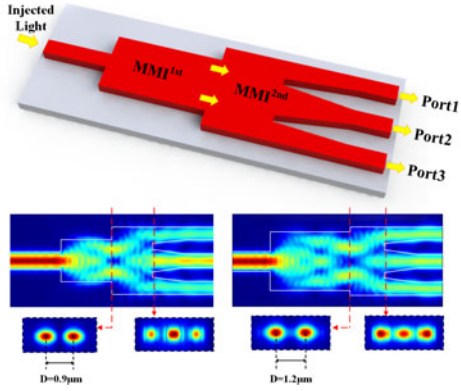

A broadband 1×3 MMI coupler with variable splitting ratios is proposed and experimentally demonstrated on SOI platform. By utilizing the structure of cascaded MMI, this kind of device has a compact footprint and high performance.

DOI: 10.1109/JPHOT.2018.2832188
1943-0655 © 2018 IEEE

IEEE photonics SOCIETY

IEEE

Broadband 1 × 3 Couplers With Variable Splitting Ratio Using Cascaded Step-Size MMI

Ye Tian,[1] Jifang Qiu,[1] Mingbin Yu,[2] Zhuili Huang,[1] Yingying Qiao,[1] Zhenli Dong,[1] and Jian Wu[1]

[1]Key Laboratory of Information Photonics and Optical Communications, Beijing University of Posts and Telecommunications, Beijing 100876, China
[2]Shanghai Institute of Microsystem and Information Technology, Chinese Academy of Sciences, Shanghai 200050, China

DOI:10.1109/JPHOT.2018.2832188

Manuscript received March 15, 2018; revised April 25, 2018; accepted April 28, 2018. Date of publication May 1, 2018; date of current version May 14, 2018. This work was supported in part by NSFC Programs under Grants 61335009, 61505011, 61475022, and 61331008, in part by 863 Program under Grant 2015AA015503, and in part by 973 Program under Grant 2014CB340100. Corresponding author: Jifang Qiu (e-mail: jifangqiu@bupt.edu.cn).

Abstract: In this paper, we propose and fabricated a novel scheme of SOI-based 1 × 3 coupler with variable splitting ratio. The coupler consists of two cascaded MMI with different sizes, and a wide range of splitting ratios from 1:0.1:1 to 1:18:1 can be achieved by modifying the size of the first-step MMI. Using the structure of cascaded step-size MMI, this kind of device has a compact footprint of below 15 μm × 15 μm and simple fabrication process. Meanwhile, the simulation analyses prove that the proposed couplers have a large operation bandwidth above 60 nm and be robust to the fabrication errors. Couplers with several splitting ratios were fabricated and well measured. Based on the measurement results, the splitting ratios of fabricated couplers from 1:0.67:1 to 1:18:1 can be achieved, and stable performance with the transmission efficiencies above 80% can be maintained over 50 nm wavelength range, which is the largest operation bandwidth to the best of our knowledge.

Index Terms: Optical couplers, silicon photonics.

1. Introduction

In recent years, photonic integrated circuits (PICs) based on Silicon-on-insulator (SOI) platform has attracted great attention due to the high level of integration density and its compatible fabrication process with integrated electronics [1]. Among the integrated components, power couplers are one of the essential items in PICs. So far, a lot of works on 1 × 2 couplers have been done and the arbitrary ratios can be achieved by a number of methods [2]–[5]. However, the research of a multi-output splitter with variable splitting ratios is still at early stage, due to the increased design complexity. A 1 × 3 coupler with variable splitting ratios would be highly advantageous for several applications, such as signal quality monitor [6], quantization resolution enhancement [7], etc. To achieve this function, various structures have been proposed, including directional couplers (DCs), photonic crystals (PhCs) [8], [9], multi-layer structures [10], QR code-like structures [11] and multimode interference (MMI) couplers. Among them, MMI couplers, which utilize the principle of self-imaging effect [12], has been considered as a preferred candidate because of its compact

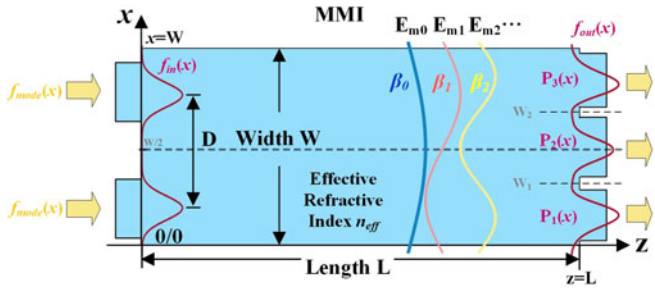

Fig. 1. Schematic of 3 Ports MMI coupler with variable splitting ratio.

footprint, wavelength insensitivity, low insertion loss and high fabrication tolerance. However, a traditional MMI usually divides the optical power equally according to the self-imaging theory, or few splitting ratios can be obtained by adjusting the positions of input and outputs ports [13]. To obtain a wide range of splitting ratios, a butterfly-shaped 1 × 3 MMI was designed and fabricated in Refs. [14]. However, the footprint is large as hundreds of microns, which may lead to the reduction of stability. MMI couplers with electro-optic tuning element is an alternative that allows the realization of tunable splitting ratios [15]. However, the footprint of this kind of device has to be large enough to avoid the thermal crosstalk, and the cost may be increased as the electro-optic tuning element requires more fabrication steps.

In this paper, we propose a novel 1 × 3 MMI coupler with variable splitting ratios. By cascading two MMI couplers of different sizes, and modifying the structure of first-step MMI, a wide range of splitting ratios can be achieved. Compared to other 1 × 3 couplers, this kind of devices have an extra compact footprint of below 15 μm × 15 μm, a large operation bandwidth above 60 nm and simple fabrication process (one-step etch). Meanwhile, the proposed couplers are robust to the fabrication errors. Then, several couplers with specific splitting ratios (from 1:0.67:1 to 1:18:1) were chosen to be fabricated on a SOI platform, the measurement results verify the high transmission efficiency of above 80% (equivalent to insertion losses below −1 dB) in a large operation bandwidth over 50 nm. Lowest insertion loss is around 0.2 dB at a wavelength of 1550 nm.

2. Principle

2.1 Analysis for Varying Splitting Ratios in MMI

For a MMI of width W and length L, according to the eigenmode decomposition theory [12], any input light distribution $f_{in}(x)$ can be decomposed into the eigenmodes in the MMI. Therefore, the output light distribution $f_{out}(x)$ is actually the superposition of each eigenmode at length L, as shown in Fig. 1. The strongly guided eigenmodes of MMI section have the form:

$$E_{mi}(x) = \sin\left((i+1)\frac{x}{W}\pi\right) \qquad \text{with } i = 0,\ 1,\ 2,\ \ldots. \tag{1}$$

where i represents the order number of eigenmodes. Using a spatial Fourier decomposition, $f_{in}(x)$ can be rewritten as a superposition of the infinite number of strongly guided eigenmodes with coefficient a_i

$$f_{in}(x) = \sum_{i=0}^{\infty} a_i E_{mi}(x), \qquad \text{with } 0 < x < W$$

$$a_i = \frac{2}{W}\int_0^W f_{in}(x)E_{mi}^*(x)dx \tag{2}$$

Thus, the output is expressed as

$$f_{out}(x) = \sum_{i=0}^{\infty} a_i E_{mi}(x) \exp(-j\beta_i L) = \sum_{i=0}^{\infty} \frac{2E_{mi}(x)}{W} \exp(-j\beta_i L) \cdot \int_0^W f_{in}(x) E_{mi}^*(x) dx \quad (3)$$

where β_i is the propagation constant for the ith order eigenmode. For a fixed operation wavelength, W, L and β_i are constants when the dimensions and material of the MMI have been defined. In this case, the only factor that affects the output is the distribution of input light.

Assuming that the fundamental mode lights $f_{\text{mode}}(x)$ are injected into the MMI section through two single mode waveguides at the positions $(W \pm D)/2$ to form the input light, where D is the distance between the input waveguides. Thus the input light distribution can be written as

$$f_{in}(x) = f_{\text{mode}}\left(x - \frac{W - D}{2}\right) + f_{\text{mode}}\left(x - \frac{W + D}{2}\right) \quad (4)$$

To obtain a MMI coupler with three output ports on SOI platform, L is selected as

$$L = \frac{1}{2} \cdot \frac{3}{4} \cdot \frac{\pi}{\beta_0 - \beta_1} - \frac{1}{3} \cdot \frac{3}{4} \cdot \frac{\pi}{\beta_0 - \beta_1} = \frac{\pi}{8(\beta_0 - \beta_1)} \quad (5)$$

where L is actually the distance between 2 self-images and 3 self-images in MMI [13]. W is given a value of 2.6 μm, in which 7 orders of eigenmodes are supported in the MMI for the convenience of calculation [16]. For an operation wavelength $\lambda = 1550$ nm, three fundamental mode lights are obtained at the output ports, referred as $P_1(x)$, $P_2(x)$ and $P_3(x)$, respectively. Therefore, the output distribution and the output power of each port (P_1, P_2, and P_3) are written as

$$f_{out}(x) = P_1(x) + P_2(x) + P_3(x)$$
$$P_1 = \int_0^{W_1} P_1(x)dx, \quad P_2 = \int_{W_1}^{W_2} P_2(x)dx, \quad P_3 = \int_{W_2}^{W} P_3(x)dx \quad (6)$$

where W_1 and W_2 are the trough positions of $f_{out}(x)$ at x axis. Since the dimensions and material of the MMI are decided, variation of D is utilized to change the distribution of $f_{in}(x)$. Correspondingly, the output distribution is changing, as shown in Fig. 2(a) that $f_{out}(x)$ changes with different D. As D increase, the value of P_2 decreases gradually, meanwhile P_1 and P_3 go increasing, which means a variable splitting ratio of three output ports can be realized by setting appropriate D.

The variations of P_1, P_2 and P_3 as a function of D from 0.55 μm to 1.65 μm are shown in Fig. 2(b). For convenience, we define the splitting index S as

$$S = \frac{P_2}{P_1 + P_2 + P_3} \times 100\% \quad (7)$$

Therefore, S is the percentage of the output power P_2. For the splitting ratios of 1:2:1 and 1:1:1, S equals to 50% and 33.3%, respectively. The splitting index S as a function of D is shown in Fig. 2(c), from where we can see that a wide range of 18% to 88% can be achieved as D varies from 0.55 μm to 1.65 μm. However, this is also the calculated splitting limitation for the device as the splitting index can hardly increase or decrease when D is less than 0.55 μm or larger than 1.65 μm, respectively.

2.2 Device Design

The 3 D schematic of our proposed device is shown in Fig. 3(a), the structure of which is named as cascade step-size MMI (CSS-MMI). It consists of two parts, one of which is referred as the first-step MMI (MMI^{1st}), with a length and a width of L_1 and W_1, respectively. The functionality of MMI^{1st} is similar to a 1 × 2 MMI, which is used to generate two single mode lights (E_1 and E_2)

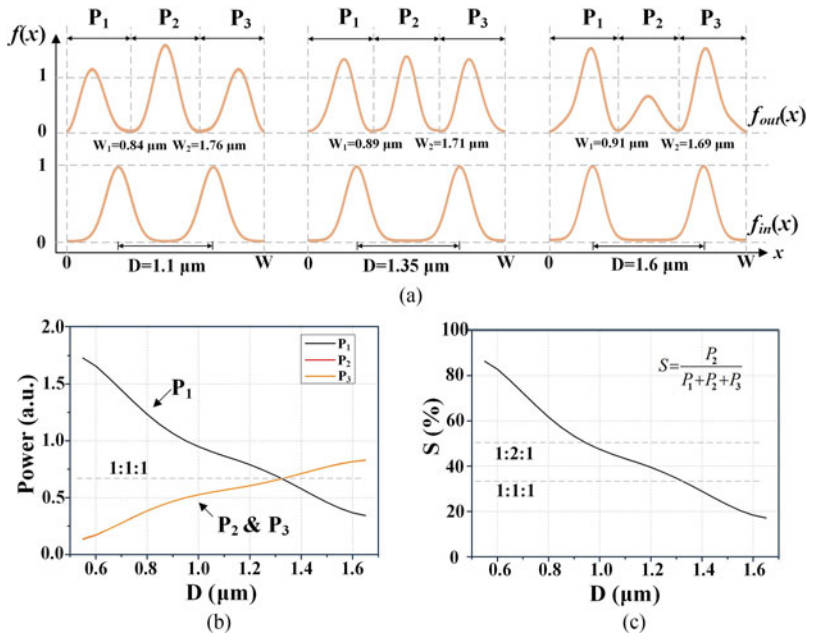

Fig. 2. (a) The output distribution $f_{out}(x)$ with different D; (b) P_1, P_2 and P_3 as a function of D; (c) Splitting index S as a function of D.

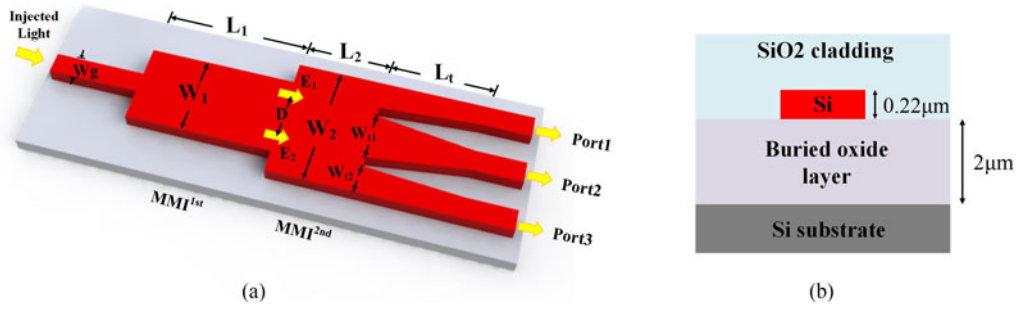

Fig. 3. (a) 3 D schematic of proposed 1 × 3 coupler. (b) Cross section of the waveguide.

with same phases for next part as two inputs. D is the distance between E_1 and E_2, and can be adjusted by modifying the dimensions of MMI^{1st}. While the other part, referred as the second-step MMI (MMI^{2nd}, with a length and a width of L_2 and W_2), is utilized to motivate a multi-modes interference and convert the two input lights into tri-outputs. Based on the principle described in above section, when D, the distance between the two inputs of MMI^{2nd}/output of MMI^{1st}, changes, a variable splitting ratio between the three outputs is obtained. The widths of input and output waveguides are both 450 nm, the tapered structure is utilized to connect the output facet of MMI^{2nd} with output ports for reducing the transmission loss. In particular, the width of middle taper is wider than others, because the middle light spot is larger than others when the splitting index is high. The whole structure is based on SOI platform with 220 nm thick-silicon layer and 2 μm thick buried oxide layer, the cross section view of the waveguides is shown in Fig. 3(b). The description and the value of main parameters of the CCS-MMI are listed in Table 1.

2.3 Simulation Results

Three-dimensional Finite-Difference Time-Domain method (3 D FDTD, Lumerical Inc.) based on SOI platform was used to simulate the performance of the proposed devices. The top view of the

TABLE 1
Main Parameters of CSS-MMI

Parameter	Value (μm)	Description
W_g	0.45	Width of input and output waveguides
L_t	2	Length of the tapers
W_{t1}	1	Width of the taper for middle Port2
W_{t2}	0.6	Width of the taper for Port1 and Port3
L_2	1.8	Length of MMI^{2nd}
W_2	2.6	Width of MMI^{2nd}
L_1	Variable	Length of MMI^{1st}
W_1	Variable	Width of MMI^{1st}
D	Variable	Distance between E_1 and E_2

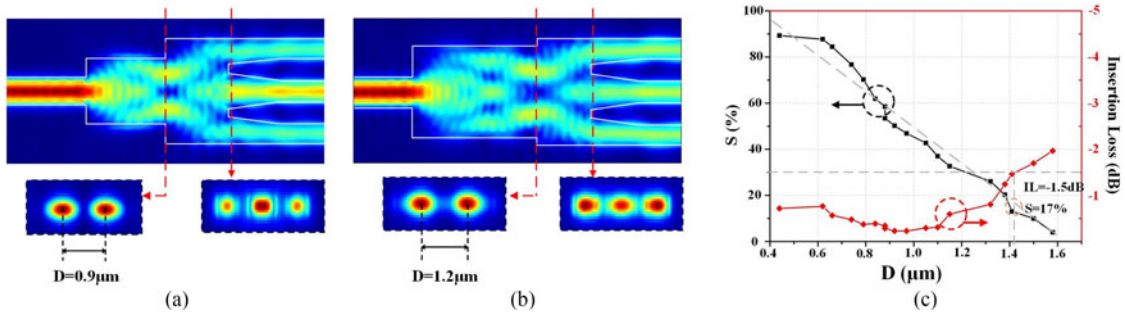

Fig. 4. Simulated optical field distributions of the CSS-MMI with splitting ratios of (a) 1:2:1 and (b) 1:1:1, the cross section view of E_1, E_2, and three outputs are shown below; (c) Variation of splitting index S and IL as a function of D.

optical transmission fields for different splitting ratios are shown in Fig. 4(a) and (b), the cross section views of E_1, E_2 and three outputs are shown below. In both cases, the lights are injected with TE polarization and the operation wavelength is $\lambda = 1550$ nm. By appropriately designing and optimizing the structures of MMI^{1st}, we have D equals to 0.9 μm and 1.2 μm respectively, and achieve splitting ratios of 1:2:1 and 1:1:1 correspondingly. Part of the sizes of MMI^{1st} and the calculated D are listed in Table 2, from where we can see that D increases as MMI^{1st} becomes larger.

By evaluating the performance of the 1 × 3 couplers with different MMI^{1st}, the variation of S and insertion loss (IL) as a function of D were obtained and are shown in Fig. 4(c). As D increases, S decreases and a wide range of splitting index from 5% to 90% are achieved. However, the IL becomes worse when D is larger than 1.1 μm or smaller than 0.9 μm, the reasons are as follow: when D increases, the sizes of light spots at Port 1 and Port 3 become larger than the taper structures as the major power is gathered on the side positions and power consumption occurs because of the reflection; when D decreases, the middle light pot becomes larger and part of the power is also reflected by the gap between the output ports. This problem can be alleviated by optimizing the size of taper structures.

TABLE 2
The Sizes of MMI[1st] and Corresponding D

D (μm)	L_1 (μm)	W_1 (μm)	D (μm)	L_1 (μm)	W_1 (μm)
0.62	1.3	1.2	1.10	3.9	2.2
0.74	1.7	1.4	1.15	4.6	2.4
0.84	2.2	1.6	1.32	5.3	2.6
0.88	2.7	1.8	1.38	6.1	2.8
0.97	3.2	2.0	1.41	6.9	3.0

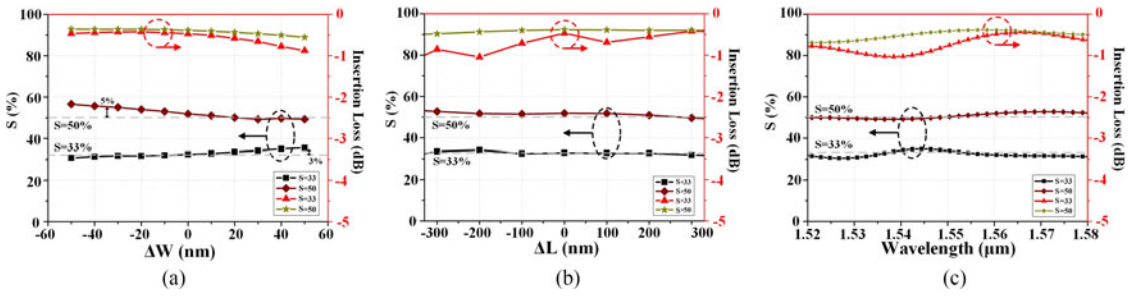

Fig. 5. S and IL of CSS-MMI as a function of (a) width deviation, (b) length deviation, and (c) operation wavelength.

Analyses of the 1 × 3 couplers with splitting index S = 33% and S = 50% are carried out to verify the robustness to the fabrication imperfections and wavelength variation. From Fig. 5(a) and (b), we can see that the variation of S is kept below 5% and the IL is less than −1 dB for both couplers by ΔW and ΔL (the variation of width and length of whole structure) of 30 nm and ±300 nm, respectively, indicating that this kind of devices are highly tolerant to the fabrication imperfections. Fig. 5(c) shows the analysis of wavelength insensitivity in a range of 60 nm, where the variation of S is still kept below 5% and the IL is less than −1 dB for both couplers.

3. Fabrication and Measurement

The proposed devices were fabricated on a SOI platform with the wafer of 220-nm top silicon layer and 2-μm buried oxide layer. 193-nm deep ultraviolet (UV) photolithography was used to define the pattern of the devices, the inductively coupled plasma (ICP) was used to etch the top Si layer with a 70 nm-thick oxide as hard mask. Spot size converters (SSCs) with tip a width of 200 nm and a length of 200 μm were integrated between the waveguides and lensed fibers to enhance the coupling efficiency, with which the coupling loss was measured to be 2 dB/facet. Finally, a silica layer of 2 μm thickness was deposited as the separate layer by plasma enhanced chemical vapor deposition (PECVD). Fig. 6(a) shows the optical micrograph of the fabricated devices, while Fig. 6(b) shows the detailed scope of the 1 × 3 CSS-MMI coupler.

Several couplers with different splitting indexes from 25% to 90% were fabricated this time, and the measured S as a function of the width of MMI[1st] is shown in Fig. 6(c), where S decreases when the width of MMI[1st] increases, matches very well with the simulation results. As for the insertion losses, most of the measured ILs are below −1 dB, which also agrees with the simulation results.

Among all the fabricated devices, three couplers with splitting indexes of 33%, 50% and 90% were selected to verify the wavelength insensitivity. For these splitting indexes, the corresponding extinction ratios (ERs) between Port 2 and Port 1 (or Port3) are supposed to be 0 dB, 3 dB and 12.5 dB, respectively. For the broadband experiment, amplified spontaneous emission (ASE) noises

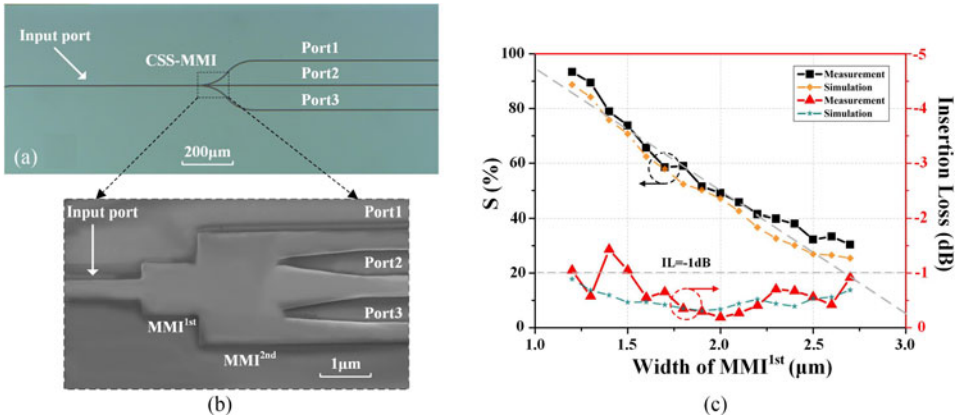

Fig. 6. (a) Optical micrograph of fabricated 1 × 3 CSS-MMI coupler. (b) SEM image of one of the couplers. (c) Measured *S* and IL as a function of the width of MMI^{1st}.

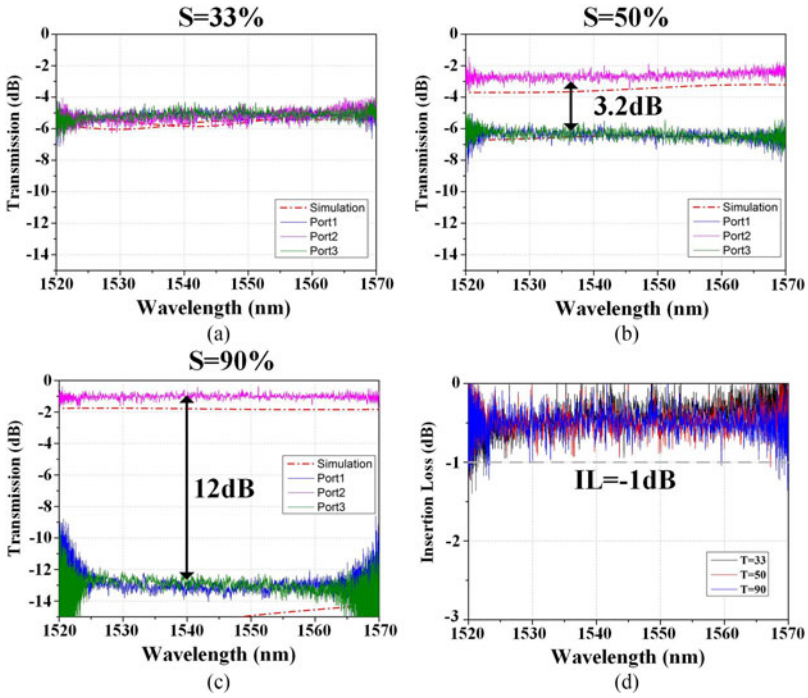

Fig. 7. The transmission spectra of the couplers with splitting indexes of (a) 33%, (b) 50% and (c) 90%. (d) The measured ILs.

from an erbium-doped fiber amplifier (EDFA) was used to be the broadband light source, and an optical spectrum analyzer (OSA) with sensitivity limitation of −70 dBm was used to measure the transmission spectrum. The measured transmission power from a reference straight waveguide was as low as ∼−40 dB, which leads to a noisy spectrum, but the source was still qualified since the OSA is quite sensitive. By injecting the noise into the devices, the transmission spectra for all the output ports are shown in Fig. 7(a)–(c), corresponding simulation results are given for comparison. We can see that the measured ERs agree well with the simulation results, and are very steady from 1520 nm to 1570 nm. Besides, as shown in Fig. 7(d), the measured ILs of all the devices are below −1 dB within the wavelength range, which means that the operation bandwidth of our proposed devices is as large as above 50 nm. However, a wavelength range wider than 50 nm cannot be measured due to the limited bandwidth of the EDFA.

4. Conclusions

We have proposed a novel scheme of a 1 × 3 MMI coupler with variable splitting ratios. By choosing appropriate dimensions of the CSS-MMI, a wide range of splitting ratios from 1:0.1:1 to 1:18:1 can be achieved. Couplers with several splitting ratios were fabricated and well measured. Based on the measured results, large operation bandwidth and high transmission efficiency of the proposed devices are achieved; experimental results agree well with the simulation results. In conclusion, this proposed device has the advantages of extra compact footprint, and robustness to the fabrication imperfections and the wavelength variation, thus it is expected to have significant applications in photonic integratable optical communication links, optical interconnection networks, and real-time signal processing systems.

References

[1] L. Thylén and L. Wosinski, "Integrated photonics in the 21st century," *Photon. Res.*, vol. 2, no. 2, pp. 75–81, 2014.
[2] D. J. Feng, T. S. Lay, and T. Y. Chang, "Waveguide couplers with new power splitting ratios made possible by cascading of short multimode interference sections," *Opt. Exp.*, vol. 15, no. 4, pp. 1588–1593, 2007.
[3] J. D. Domenech, J. S. Fandino, and B. Gargallo, "Arbitrary coupling ratio multimode interference couplers in silicon-on-insulator," *J. Lightw. Technol.*, vol. 32, no. 14, pp. 2536–2543, Jul. 2014.
[4] Q. Deng, L. Liu, X. Li, and Z. Zhou, "Arbitrary-ratio 1 × 2 power splitter based on asymmetric multimode interference," *Opt. Lett.*, vol. 39, no. 19, pp. 5590–5593, 2014.
[5] M. Cherchi, S. Ylinen, M. Harjanne, M. Kapilainen, T. Vehmas, and T. Aalto, "Unconstrained splitting ratios in compact double-MMI couplers," *Opt. Exp.*, vol. 22, no. 8, pp. 9245–9253, 2014.
[6] J. Qiu, Y. Tian, Z. Huang, Y. Wang, D. Kong, and J. Wu, "Integrated in-band OSNR monitor based on asymmetrical parallel-MZIs for WDM signals," *IEEE J. Sel. Topics Quantum Electron.*, vol. 22, no. 6, pp. 467–472, Nov./Dec. 2016.
[7] Z. Kang *et al.*, "Resolution-enhanced all-optical analog-to-digital converter employing cascade optical quantization operation," *Opt. Exp.*, vol. 22, no. 18, pp. 21441–21453, 2014.
[8] M. Zhang, R. Malureanu, A.C. Kruger, and M. Kristensen, "1 × 3 beam splitter for TE polarization based on self-imaging phenomena in photonic crystal waveguides," *Opt. Exp.*, vol. 18, no. 14, pp. 14944–14949, 2010.
[9] D. Zhuang *et al.*, "1 × 3 optical drop splitter in a rod-type silicon photonic crystal," in *Proc. Asia Commun. Photon. Conf. Exhib.*, Shanghai, China, vol. 41, 2012, pp. 311–315.
[10] K. Shang *et al.*, "Silicon nitride tri-layer vertical Y-junction and 3D couplers with arbitrary splitting ratio for photonic integrated circuits," *Opt. Exp.*, vol. 25, no. 9, pp. 10474–10483, 2017.
[11] K. Xu *et al.*, "Integrated photonic power divider with arbitrary power ratios," *Opt. Lett.*, vol. 42, no. 4, pp. 855–858, 2017.
[12] M. Bachmann, P. A. Besse, and H. Melchior, "General self-imaging properties in n × n multimode interference couplers including phase relations," *Appl. Opt.*, vol. 33, no. 18, pp. 3905–3911, 1994.
[13] M. Bachmann, P. A. Besse, and H. Melchior, "Overlapping-image multimode interference couplers with a reduced number of self-images for uniform and nonuniform power splitting," *Appl. Opt.*, vol. 34, no. 30, pp. 6898–6910, 1995.
[14] P. A. Besse, E. Gini, M. Bachmann, and H. Melchior, "New 2 × 2 and 1 × 3 multimode interference couplers with free selection of power splitting ratios," *J. Lightw. Technol.*, vol. 14, no. 10, pp. 2286–2293, Oct. 1996.
[15] C. H. Joyner and J. Leuthold, "Multimode interference couplers with tunable power splitting ratios," *J. Lightw. Technol.*, vol. 19, no. 5, pp. 700–707, May 2001.
[16] D. Dai, J. Wang, and Y. Shi, "Silicon mode (de)multiplexer enabling high capacity photonic networks-on-chip with a single-wavelength-carrier light," *Opt. Lett.*, vol. 38, no. 9, pp. 1422–1424, 2013.